Changing direction: influence of ligand electronics on the directionality and kinetics of photoinduced charge transfer in Cu(I)diimine complexes

Journal:	*Inorganic Chemistry*
Manuscript ID	ic-2023-02043n.R1
Manuscript Type:	Article
Date Submitted by the Author:	n/a

Complete List of Authors:	Wang, Lei; University of Shanghai for Science and Technology, School of Materials and Chemistry Xie, Zhu-Lin; Argonne National Laboratory, Chemical Sciences and Engineering Phelan, Brian; Northwestern University, Lynch, Vincent; University of Texas at Austin, Chemistry Chen, Lin; Argonne National Laboratory, Chemical Sciences and Engineering ; Northwestern University, Department of Chemistry Mulfort, Karen; Argonne National Laboratory, Chemical Sciences and Engineering

Changing direction: influence of ligand electronics on the directionality and kinetics of photoinduced charge transfer in Cu(I)diimine complexes

Lei Wang,[a, b] Zhu-Lin Xie,[a] Brian T. Phelan,[a] Vincent M. Lynch,[c] Lin X. Chen,[a,d] Karen L. Mulfort*[a]

[a]Argonne National Laboratory, Division of Chemical Sciences and Engineering, Lemont, IL 60439; [b]University of Shanghai for Science and Technology, School of Materials and Chemistry, Shanghai 200093, China; [c]University of Texas Austin, Department of Chemistry, Austin, TX, 78712; [d]Northwestern University, Department of Chemistry, Evanston, IL 60208

ABSTRACT: A key challenge to the effective utilization of solar energy is to promote efficient photoinduced charge transfer, specifically avoiding unproductive, circuitous electron-transfer pathways and optimizing the kinetics of charge separation and recombination. We hypothesize that one way to address this challenge is to develop the fundamental understanding of how to initiate and control *directional* photoinduced charge transfer, particularly for earth-abundant first-row transition metal coordination complexes which typically suffer from relatively short excited-state lifetimes. Here we report a series of functionalized heteroleptic copper(I)bis(phenanthroline) complexes which have allowed us to investigate the directionality of intramolecular photoinduced metal-to-ligand charge transfer (MLCT) as a function of substituent Hammett parameter. Ultrafast transient absorption suggests a complicated interplay of MLCT localization and solvent interaction with the Cu(II) center of the MLCT state. This work provides a set of design principles for directional charge transfer in earth-abundant complexes and can be used to efficiently design pathways for connecting the molecular modules to catalysts or electrodes, and integration into systems for light-driven catalysis.

Introduction

Understanding where photogenerated electronic excited states localize and how long they persist is of fundamental, critical importance for the effective and efficient conversion of diffuse solar energy to that stored as electricity and chemical fuels,[1] as well as developing advanced schemes for selective photoredox catalysis.[2-3] Transition metal coordination complexes present a particularly useful platform to advance this understanding as they span a rich diversity in molecular structure that enables a wide range of optical and electronic properties in their ground and excited states.[4-6] Our group[7-9] and others[10-12] have focused specifically on earth-abundant copper(I)diimine complexes as molecular photosensitizers because of their promising photophysical properties and ability to participate in excited-state redox chemistry.[13-17] In particular, heteroleptic Cu(I)diimine complexes with their asymmetric coordination environment present an ideal platform to investigate directional, intramolecular photoinduced charge transfer. The heteroleptic phenanthroline (HETPHEN) approach developed by Schmittel and co-workers[18-20] allows the synthesis of stable and analytically pure asymmetric Cu(I)bis(phenanthroline) complexes using two different phenanthroline ligands, avoiding complications arising from the relatively labile Cu(I)—N coordination.[21] Further, the four-coordinate, ideally tetrahedral geometry of a $3d^{10}$ Cu(I) center presents a linear arrangement of ligand substituents and removes the possibility of positional or stereoisomers common for octahedrally-coordinated complexes that can complicate spectroscopic analyses.[11] Our group and others have used the asymmetric coordination environment of the HETPHEN platform to investigate directional photoinduced charge-transfer pathways[11, 22-26] and targeted surface immobilization schemes.[27-28]

Early systematic structure-activity investigations of homoleptic Cu(I)diimine complexes revealed that their coordination environment is quite flexible and susceptible to a large flattening distortion upon visible photoexcitation and metal-to-ligand charge-transfer (MLCT) in the formal Cu(II) oxidation state.[12, 29-30] This excited-state reorganization is highly responsive to ligand structure and solvent environment, but can give rise to very short excited-state lifetimes.[31] Therefore, much of the work to modulate the ground- and excited-state properties of Cu(I)bis(phen) complexes in particular has focused on investigating the impact of ligand steric effects, primarily at the 2,9-phenanthroline position adjacent to the coordinating nitrogen atoms.[31-36]

In contrast to the extensive literature on the effect of ligand sterics on the ground- and excited-state properties of Cu(I)bis(phen) complexes, a glaring knowledge gap for these molecular photosensitizers is any systematic investigation of how electron-donating or -withdrawing substituents can be used to tune, and ultimately predict, their ground- and excited-state properties. Here we describe several new heteroleptic Cu(I)bis(phenanthroline) (CuHETPHEN) complexes

functionalized with electron-donating and -withdrawing groups with a wide range of Hammett constants (-0.37 < σ_p < 0.6), shown in **Figure 1**. In this study we have observed a linear relationship between the Cu(II/I) oxidation potential and σ_p of the ligand substituents, demonstrating a strategy to precisely tune the electrochemical properties of these complexes. The UV-Vis spectra for all complexes are closely reproduced by time-dependent density functional theory (TD-DFT) calculations that provide insight into how the 4,7-R-phen substitution directs the MLCT transition between the two different ligands. The excited-state kinetics of the series of complexes are dictated by solvent environment, like what is known for other Cu(I)bis(phen) complexes. However, we observe a non-linear response of the ^{3}MLCT decay as a function of σ_p, which is different for non-coordinating and coordinating solvents. The results presented here demonstrate the implementation of electronic molecular structure factors in tandem with solvent environment to tune and predict the properties and excited-state dynamics of these earth-abundant molecular photosensitizers.

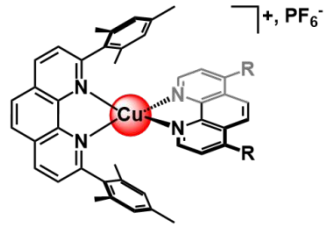

[Cu(mesphen)(4,7-R-phen)](PF$_6$)

Complex	R	σ_P
Cu-OH	OH	-0.37
Cu-OCH_3	OCH_3	-0.27
Cu-CH_3	CH_3	-0.17
Cu-H	H	0
Cu-Br	Br	0.23
Cu-CHO	CHO	0.42
Cu-PO_3Et_2	PO_3Et_2	0.60

Figure 1. Chemical structure of CuHETPHEN complexes studied in this work, abbreviated as **Cu-R**, and σ_p values of the 4,7-R-phenanthroline substituents.

Results and Discussion

Synthesis and molecular structure characterization

The HETPHEN synthesis approach developed by Schmittel and co-workers[18-20] first introduces one equivalent of a phenanthroline ligand with extreme 2,9-steric bulk, typically 2,9-dimesityl-1,10-phenanthroline (mesphen), to a solution of Cu(I). A single Cu(I) center cannot bind another mesphen ligand and therefore addition of one equivalent of a second phen ligand yields an analytically pure and stable Cu(I)diimine complex with two different ligands, which is not possible without the steric bulk of mesphen because of the coordinative lability of Cu(I)diimine complexes. Using the HETPHEN approach, our group has reported several variations of steric bulk of both ligands, and benchmarked the ground- and excited-state properties.[8-9]

Seven stable CuHETPHEN complexes formulated as [Cu(mesphen)(4,7-R-phen)]PF_6 (where 4,7-R-phen = 4,7-R-1,10-phenanthroline, abbreviated as **Cu-R**), were obtained using the one-pot, two-step synthesis procedure originally described by Schmittel and co-workers.[18-20, 37] Except for **Cu-H**,[8] these **Cu-R** complexes have not been previously reported, and detailed synthetic procedures and full structural characterization are described in the Supporting Information. All complexes were prepared in anhydrous de-aerated dichloromethane except **Cu-OH**, which was synthesized in anhydrous deaerated methanol because of the poor solubility of 4,7-OH-1,10-phenanthroline in dichloromethane. The ^{1}H NMR, ^{13}C NMR, mass spectra, and elemental analysis are consistent with the molecular structures shown in **Figure 1** and confirm no formation of the homoleptic analogs (**Figures S3-S16**). During the routine characterization of **Cu-CHO**, we observed that its ^{1}H NMR spectrum in deuterated methanol demonstrates peak shifts and splitting that are inconsistent with the expected structure and the spectra in other solvents, and confirmed that the aldehyde is converted to a stable hemiacetal species in hydroxyl-containing solvents. A full description of this process is outside the scope of the current study and will be the topic of an upcoming manuscript; no further studies of **Cu-CHO** were performed in hydroxyl-containing solvents.

Single crystal X-ray structural characterization

The heteroleptic coordination and geometry of the **Cu-R** complexes were confirmed by single crystal X-ray diffraction, with the exception of **Cu-OH** because its crystals degraded at the operating temperature of the diffractometer (**Cu-H** was reported previously by our group[8]). The single crystal X-ray structures of **Cu-OCH_3** and **Cu-PO_3Et_2**, which contain representative electron-donating and –withdrawing groups, are shown in **Figure 2** and all other **Cu-R** complexes are shown in **Figures S17-S23**. The crystallographic data are summarized in **Table S1** and selected interatomic bond lengths and angles are listed in **Tables 1** and **S2**. **Cu-Br** and **Cu-CHO** crystallize in the space group $P2_1/c$, and **Cu-OCH_3**, **Cu-CH_3** and **Cu-PO_3Et_2** crystallize in the space group P-1. The asymmetric unit for **Cu-OCH_3** and **Cu-PO_3Et_2** is occupied by one **Cu-R** molecule, and that of **Cu-Br** and **Cu-CHO** is occupied by one **Cu-R** molecule and one molecule of dichloromethane solvent. The asymmetric unit of **Cu-CH_3** is occupied by two independent molecules.

Most of the studied complexes show the "pac-man" motif due to preferential π–π interaction between one mesityl group of mesphen and the B-ring of the secondary phenanthroline ligand which leads to considerable distortion from tetrahedral geometry at the Cu(I) center.[38] However, the bulky phosphonate esters on complex **Cu-PO_3Et_2** result in the phenanthroline positioned in the middle of the mesityl groups and form a "centered" motif. The coordination geometry of the Cu(I) center of the new **Cu-R** complexes was quantified using the geometry index parameter s_4 which ranges from s_4 = 1 for perfect tetrahedral coordination to s_4 = 0 for square planar geometry.[39] Analysis of the **Cu-PO_3Et_2** crystal structure reveals a smaller distortion from tetrahedral geometry (s_4 = 0.734) in comparison to the other complexes reported here (s_4 = 0.66-0.68) and previously described CuHETPHEN crystal structures.[8-9] Major differences in ground-state structure such as this are typically thought to arise from variation in the steric bulk at the 2,9-phenanthroline position but here we observe that the bulky phosphonate ester groups over 6 Å from the Cu(I) center also have a considerable impact on its geometry.

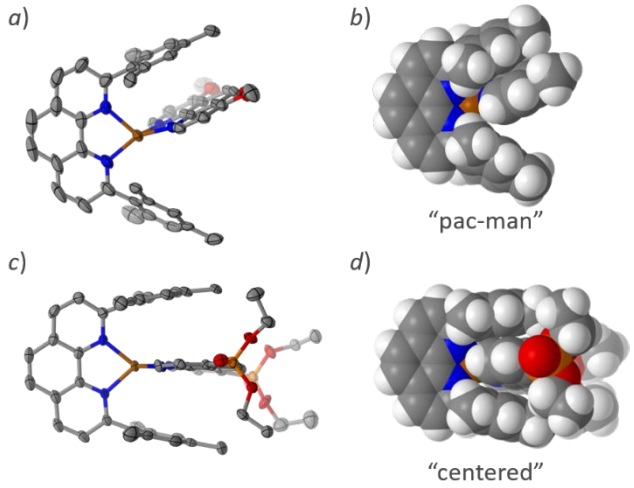

Figure 2. Perspective view of a) **Cu-OCH$_3$** and c) **Cu-PO$_3$Et$_2$** (50% probability ellipsoids). Carbon, gray; nitrogen, blue; oxygen, red; phosphine, orange; copper, brown. The PF_6^- counterion, solvent molecule, and hydrogen atoms are omitted for clarity. Space-filling diagrams of b) **Cu-OCH$_3$** and d) **Cu-PO$_3$Et$_2$**, illustrating "pac-man" and "centered" interactions between hetero-ligands coordinated to Cu(I).

Table 1. Selected Bond Length, Bond Angles, and Geometry Index Parameter s_4 for representative **Cu-R**.

Complex	Cu-OCH$_3$	Cu-H	Cu-PO$_3$Et$_2$
Selected bond lengths			
Cu1–N1[a]	1.979(2)	2.068(5)	2.025(4)
Cu1–N2[a]	2.095(2)	2.046(7)	2.028(4)
Cu1–N3[b]	1.995(2)	2.027(6)	2.009(4)
Cu1–N4[b]	2.044(3)	2.060(7)	2.014(4)
Selected bond angles			
N1–Cu1–N2	81.40(10)	81.2(2)	82.94(15)
N1–Cu1–N3	141.66(11)	113.9(2)	118.51(16)
N1–Cu1–N4	125.23(10)	119.7(3)	132.25(15)
N2–Cu1–N3	118.88(9)	126.4(3)	124.25(15)
N2–Cu1–N4	106.56(9)	136.5(2)	123.53(15)
N3–Cu1–N4	82.39(9)	82.2(2)	82.21(15)
s_4 values	0.660	0.689	0.734

[a] N1 and N2 are the N atoms of the mesphen ligand. [b] N3 and N4 are the N atoms of 4,7-R-phen.

Electrochemical analysis

The electrochemical behavior of the **Cu-R** series was measured by cyclic voltammetry and square wave voltammetry in dichloromethane, methanol, acetone, and dimethylformamide (**Figures 2a** and **S24-S29**, summarized in **Tables S3** and **S4**). The Cu(II/I) redox potential shifts anodically with increasing σ_p of the substituents on the secondary phen ligand, which aligns with our expectations that increasing the electron-withdrawing ability of the substituents reduces the electron density of the Cu(I) center, creating a metal center which is more difficult to oxidize. Of the series, **Cu-PO$_3$Et$_2$** which contains the strongest electron withdrawing group (σ_p = 0.6) was oxidized at the highest potential (439 mV vs. Fc/Fc^+ in dichloromethane) and complex **Cu-OH** with the strongest electron-donating group (σ_p = -0.37) was oxidized at the lowest potential (96 mV vs. Fc/Fc^+ in dichloromethane). Most of the studied CuHETPHEN complexes are relatively well-behaved with reversible Cu(II/I) couples in the non-coordinating solvent dichloromethane, with the exception of **Cu-PO$_3$Et$_2$** which displays a peak-to-peak ΔE of 105 mV. Not only do the phosphonate ester groups have the greatest electron withdrawing character, but they also enforce a more tetrahedral geometry at the Cu(I) center than the other complexes, as seen in the large s_4 value calculated from the crystal structure. The preferred flattened geometry of the oxidized copper center is likely more difficult to achieve with the steric bulk of the phosphonate ester substituents. It is a well-documented trend that for homoleptic Cu(I)diimine complexes increasing the steric bulk at the 2,9-phen position, adjacent to the Cu(I)-coordinating nitrogen atoms, dramatically increases the Cu(II/I) oxidation potential because of the increased resistance to the flattening distortion in the Cu(II) state.[31] Here we propose that the bulky phosphonate ester groups in the second coordination sphere also promotes steric resistance to oxidation. As previously observed for CuHETPHEN complexes with 2,9-H substitution on the secondary phen ligand, the Cu(II/I) couples measured here show some non-ideal behavior in the coordinating solvents methanol, acetone, and DMF (**Figures S24-S29**).

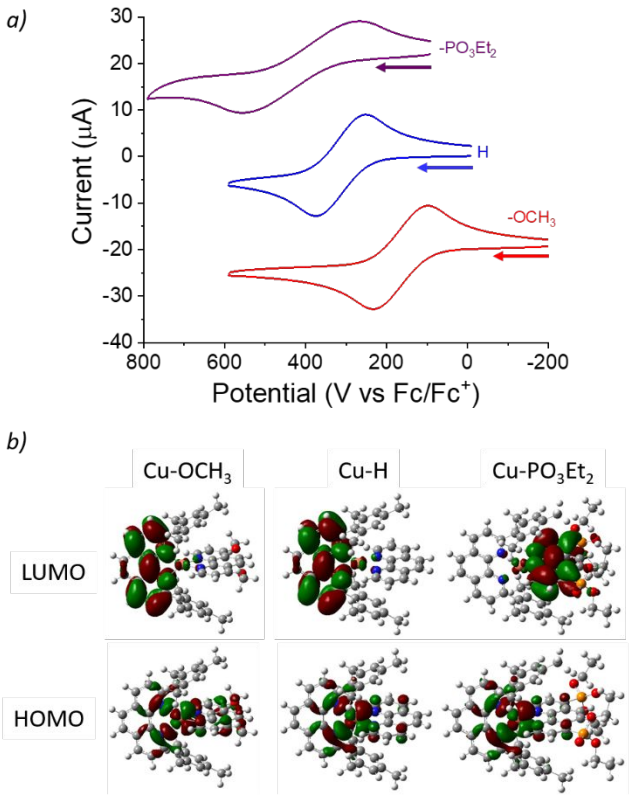

Figure 3. (a) Comparison of the cyclic voltammograms of 1 mM **Cu-OCH$_3$**, **Cu-H**, and **Cu-PO$_3$Et$_2$** in dichloromethane containing 0.1 M NBu_4PF_6 with a glassy carbon working electrode. Arrows

indicate scan direction. (b) DFT-calculated HOMO and LUMO orbitals for **Cu-OCH$_3$**, **Cu-H**, and **Cu-PO$_3$Et$_2$**.

A prime motivation for preparing and investigating this series of **Cu-R** complexes was to understand the role of the electronic effect for predicting and directing their electronic and photophysical properties. As previously reported,[40-43] the Hammett free-energy equation is widely used to establish relationships between the effect of substituents and ground state molecular properties, as shown in equation (1):

$$E_{1/2}(L) = \rho\sum\sigma + E_{1/2}(H) \quad (1)$$

where $\sum\sigma = 2 \times \sigma_p$ and in our case, $E_{1/2}(H)$ is a constant and ρ is a reaction-dependent constant. Therefore, a simplified equation to correlate the Cu(II/I) potential with the Hammett parameter of the 4,7-R-phen substitution is shown in equation (2):

$$E_{1/2}(L) \propto \sigma_p \quad (2)$$

Treatment of the Cu(II/I) couples obtained by cyclic voltammetry using this approach reveals a strong correlation between E and σ_p in dichloromethane, acetone, methanol, and DMF (**Figure S27** and **S29**), and agrees with trends previously established for other coordination complexes.[44] This demonstrates the effect of the electron-donating or -withdrawing ability of the 4,7-R-phen substituents on the metal-centered oxidation potential of the **Cu-R** complexes, enabling a predictive framework for yet to be synthesized complexes.

The complete electrochemical potential window for the **Cu-R** complexes was measured in dichloromethane and dimethylformamide to test our hypothesis that the electron-donating or –withdrawing groups would impact the ligand reduction potential in addition to the Cu(II/I) oxidation (**Figure S28**). For **Cu-R** with electron-donating substitution ($-0.37 < \sigma_p < 0$), we observe that the first and only ligand reduction observed within the solvent potential window occurs between -2.1 – -2.2 V vs. Fc/Fc$^+$, which we assign to the mesphen ligand as it aligns with the potential observed for the ligand alone in solution. For **Cu-R** with electron-withdrawing substituents ($0 < \sigma_p < 0.6$) the observed reduction potential shifts to more positive values, ranging from -1.5 – -1.8 V vs. Fc/Fc$^+$. Taking these observations together we conclude that the lowest energy ligand reduction is on the mesphen ligand for **Cu-R** with ($-0.37 < \sigma_p < 0$) and on the 4,7-R-phen ligand for **Cu-R** with $\sigma_p > 0$.

To further understand how the ligand substitution impacts molecular electronic structure, DFT calculations were performed using the B3LYP/LanL2DZ functional/basis-set. The HOMO of each **Cu-R** complex primarily arises from the 3d orbital of the copper center with σ* character from the Cu-N antibonding orbitals and contributions from the N, the σ-donor orbitals of one ligand. Additionally, it also indicates an involvement of dπ-Lπ* interaction with the secondary ligand.. The LUMO are π* orbitals localized on the mesphen ligand for **Cu-R** with electron-donating groups, but π* orbitals localized on the 4,7-R-phen ligand for **Cu-R** with electron-withdrawing groups (**Figure 3b** and **Figure S31**). This supports the experimental cyclic voltammetry, and is a clear demonstration of the effect of the electron-withdrawing groups decreasing the energy of the phen ligand so that the LUMO is localized on the π* orbital in that ligand.

UV-Vis absorbance spectra and TD-DFT calculations

The UV-Vis absorption spectra of **Cu-R** were measured in dichloromethane, methanol, and acetone at room temperature (**Figures 4** and **S30**, summarized in **Table S5**). All **Cu-R** have identical 2,9-phenanthroline substitution, which is known to have considerable influence on the MLCT energy and intensity,[7, 10] so here we can focus instead on the impact of the 4,7-R-phen substitution. The complexes with $-0.37 < \sigma_p < 0.23$ all exhibit a broad absorption band centered between 463 - 472 nm with extinction coefficients in the $4000 < \varepsilon < 8000$ M^{-1}cm^{-1} range, consistent with other CuHETPHEN complexes with similar 2,9-phenanthroline substitution.[8-9] Following from the Cu(I)diimine literature, we assign this band to MLCT from Cu(I) to the phenanthroline ligands.[31] The DFT calculations (**Figures 3b** and **S31**) indicate that MLCT occurs toward the mesphen ligand for **Cu-H** and those with electron donating groups, and the electron donors shift the MLCT transition to slightly higher energy. Conversely, **Cu-PO$_3$Et$_2$** with the most strongly electron-withdrawing substituents ($\sigma_p = 0.6$) has the lowest energy MLCT band of the series, with a ~30 nm red-shifted MLCT band compared to the other **Cu-R**.

To better understand the observed **Cu-R** absorption spectra, we calculated the electronic spectra by TD-DFT analysis using the DFT optimized geometries (full details in the Supporting Information). We performed the calculations on isolated **Cu-R** cations with the polarizable continuum model to simulate solvent effects, and natural transition orbitals (NTOs) based on the TD-DFT calculations were generated to visualize the dominant transitions (oscillator strength $f \geq 0.02$).[45-46] The choice of computational parameters is supported by good agreement between the measured and computed spectra (**Figures S32**-**S44**). Bands located in the high-energy region (250 - 350 nm) are attributed to the π–π* electronic transitions of the phen ligands, and the spectral features in the low-energy region (400 - 550 nm) are assigned to MLCT. The long-wavelength shoulder between 520 – 650 nm observed in the experimental spectra (**Figure 4**) is not captured at the level of TD-DFT calculations used here. However, this low energy shoulder for these complexes is well understood, and typically assigned to transitions to the S_1 state that are formally symmetry forbidden but gain intensity via distortions from tetrahedral geometry.[7]

Comparison of the TD-DFT calculated MLCT band assignments and experimentally observed transitions for **Cu-OCH$_3$**, **Cu-H**, and **Cu-PO$_3$Et$_2$** are presented in Table 2, as representative **Cu-R** across this Hammett series. For **Cu-OCH$_3$**, the weak shoulder band at ~400 nm arises from MLCT transition between dπ(Cu) → π*(phen-OCH$_3$) but the dominant MLCT band at ~451 nm is primarily dπ(Cu) → π*(mesphen) in character. The largest intensity MLCT band for **Cu-H** at 465 nm shows roughly equal character from charge transfer to both ligands, dπ(Cu) → π*(phen) and dπ(Cu) → π*(mesphen). And for **Cu-PO$_3$Et$_2$** with the strongest electron-withdrawing groups in this series, the

dominant MLCT band at 482 nm is characterized by dπ(Cu) → π*(phen-PO_3Et_2). Comparing the TD-DFT calculations across the series demonstrates how MLCT moves from one ligand to the other directed by the 4,7-R-phen substitution.

Examination of the experimentally observed and calculated spectra demonstrate that the nature of the MLCT transition is fundamentally different between the **Cu-R** with electron-donating groups and those with electron-withdrawing groups. For **Cu-R** with electron-donating groups (-0.37 < σ_p < 0), the peak of the MLCT bands fall within a very narrow range. In this subset of **Cu-R**, the experimental values only vary by 5 nm in all solvents investigated (Table S5) and the TD-DFT calculated values only differ by 1 nm (Tables S6, S7). This near equivalence in MLCT energy strongly suggests that MLCT is localized on the same ligand for each of these complexes, and the TD-DFT calculations point to the mesphen ligand. By contrast, the experimental and calculated range of MLCT maxima for **Cu-R** with 0 < σ_p < 0.6 is approximately 30 nm. This large difference in MLCT energy among the **Cu-R** with electron-withdrawing groups indicates that MLCT occurs on the ligand with different electronic structure induced by the 4,7-phen substituents. Comparing the two sets of **Cu-R** complexes supports the directionality of initial MLCT.

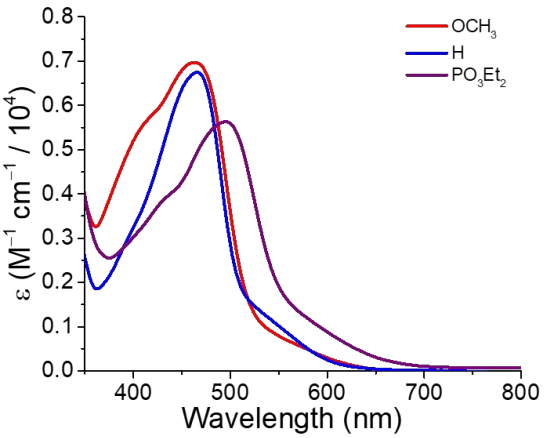

Figure 4. Comparison of the UV-Vis absorbance spectra of **Cu-OCH_3**, **Cu-H**, **Cu-PO_3Et_2** in dichloromethane.

Table 2. Comparison of TD-DFT calculated absorption maxima (in nm) for with experimental results for **Cu-OCH_3**, **Cu-H**, and **Cu-PO_3Et_2** in dichloromethane, for major transitions related to MLCT.

Expt	Calc	Transition	f	P
		Cu-OCH_3		
403	400	dπ(Cu) → π*(phen-OCH_3)	0.028	0.983
464	455	dπ(Cu) → π*(mesphen)	0.128	0.885
		Cu-H		
401	414	dπ(Cu) → π*(mesphen)	0.025	0.974
465	455	dπ(Cu) → π*(phen)	0.114	0.518
465	455	dπ(Cu) → π*(mesphen)	0.114	0.456
		Cu-PO_3Et_2		
427	414	dπ(Cu) → π*(mesphen)	0.034	0.836
495	482	dπ(Cu) → π*(phen-PO_3Et_2)	0.149	0.867

Transient absorption spectroscopy

Ultrafast transient absorption (TA) spectroscopy was used to quantify the excited-state kinetics of **Cu-R** in dichloromethane (**Figure 5**, **S45-S52**) and dimethylformamide (**Figures S53-59**). Following 415 nm excitation a ground state bleach centered at ~460 nm was immediately observed in conjunction with a broad excited-state absorption centered at 560 nm for all **Cu-R**. The broad excited-state absorption feature transitions to a double headed feature that is assigned to the vibronic features of the phenanthroline radical anion in the ^{3}MLCT state, shown for **Cu-OCH_3** in CH_2Cl_2 in **Figure 5A** and **Figures S45-S59** for all other complexes. Comparing the transient spectra at one time delay across the **Cu-R** series reveals another piece of evidence to support the directionality of MLCT. **Figure S60** shows that that the maximum of the excited state absorption feature for **Cu-R** with electron-donating groups (-0.37 < σ_p < 0) fall within a very narrow range, between 573 – 576 nm, suggesting that the excited state for all these complexes has the same electronic structure and is localized on the mesphen ligand which is common to all the **Cu-R**. By contrast, the MLCT maximum intensity for **Cu-R** with electron-withdrawing groups (0 < σ_p < 0.6) are substantially blue-shifted with respect to **Cu-H** (559 nm for **Cu-Br** and 553 nm for **Cu-PO_3Et_2**), and span a wider range. This indicates that the MLCT state is localized on the secondary ligand that has a different electronic structure for each **Cu-R**, arising from the 4,7-phen substituents. Similar to our analysis of the steady-state absorption spectra, the trend in excited state absorption spectra point to a localized MLCT state that switches from the mesphen ligand for **Cu-R** with electron-donating groups to the 4,7-R-phen ligand for **Cu-R** with electron-withdrawing groups.

The excited-state kinetics for all **Cu-R** were modeled using a tri-exponential decay function convolved with a Gaussian instrument response function via global kinetic analysis of several probe wavelengths (**Figure 5B**, summarized in **Tables 3** and **S7**). Following from literature precedent,[7, 47] we assign the shortest time component $\tau_1$to the Jahn-Teller (flattening) distortion in the ^{1}MLCT Cu(II) excited state, the second time component τ_2 to intersystem crossing (ISC) from ^{1}MLCT to ^{3}MLCT, and the final decay component τ_3 to ^{3}MLCT decay and ground-state recovery. In the initial unconstrained fits, the τ_1 values obtained for some **Cu-R** in CH_2Cl_2 and all in DMF were much shorter than the ~0.3 ps instrument response of our transient absorption set-up and are therefore reported as < 0.3 ps. In these cases we fixed the value for τ_1 to 0.3 ps as an upper limit of the flattening distortion process and allowed τ_2 and τ_3 to fit the data completely unconstrained.

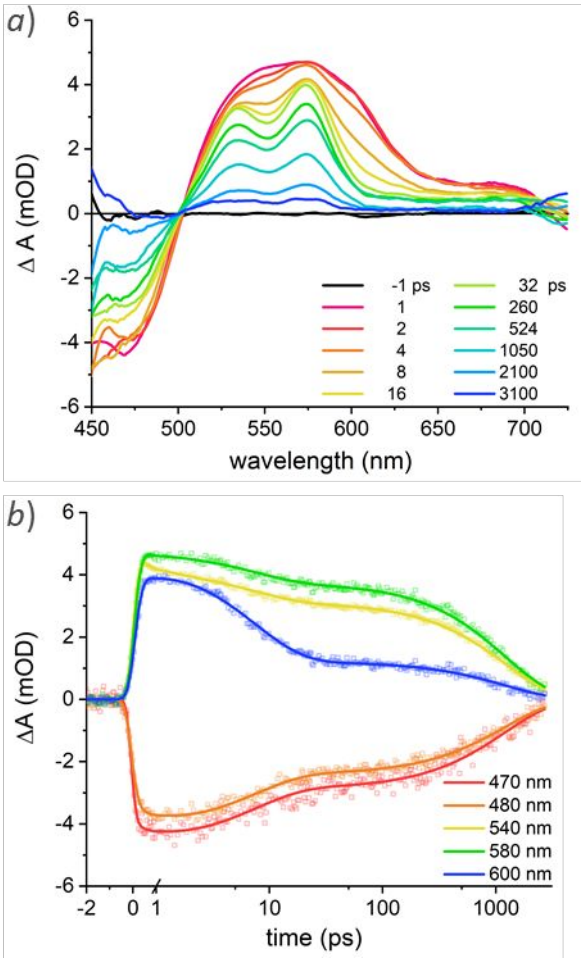

Figure 5. Ultrafast transient absorption spectroscopy of **Cu-OCH$_3$** in CH_2Cl_2 following 415 nm excitation. a) Transient spectra with delay times noted in legend. b) Global fit of excited-state kinetics at five wavelengths corresponding to ground-state bleach and excited-state absorption. Data in square points, fits in corresponding lines.

The ultrafast kinetics for the **Cu-R** series as a function of solvent donating ability are aligned with previously described excited-state dynamics of Cu(I)diimine complexes. In general for Cu(I)bis(phen) complexes, the ^{3}MLCT decay τ_3 is highly solvent-dependent because coordinating solvent molecules can interact with the Cu(II) center in the flattened MLCT geometry and accelerate ^{3}MLCT decay as compared to that in non-coordinating solvents.[7] Therefore, as expected, the τ_3 values for **Cu-R** that correspond to ^{3}MLCT decay are between four and two hundred times shorter in coordinating DMF than in CH_2Cl_2.

Table 3. Summary of excited-state kinetics for **Cu-R** following 415 nm excitation in CH_2Cl_2 and DMF.

Cu-R	CH_2Cl_2		DMF	
	τ_2 (ps)	τ_3 (ps)	τ_2 (ps)	τ_3 (ps)
Cu-OH	8.8 ± 0.2	1010 ± 10	6.5 ± 0.4	230 ± 4
Cu-OCH_3	7.5 ± 0.2	1212 ± 10	4.8 ± 0.3	246 ± 2
Cu-CH_3	9.9 ± 0.4	2020 ± 30	6.6 ± 0.3	215 ± 1
Cu-H	10.2 ± 0.5	3490 ± 40	7.2 ± 0.3	146 ± 1
Cu-Br	10.4 ± 0.2	3250 ± 50	3.0 ± 0.3	19.8 ± 0.3
Cu-CHO	3.3 ± 0.2	200 ± 10	0.9 ± 0.3	12.4 ± 0.3
Cu-PO_3Et_2	7.8 ± 0.2	1410 ± 10	2.7 ± 0.3	18.4 ± 0.3

In contrast to the expected solvent dependence for the kinetics of the **Cu-R** series, the 4,7-phen substituents produce a surprising, non-linear correlation of τ_3 in response to σ_p, and this correlation is different in non-coordinating CH_2Cl_2 than for coordinating DMF (**Figure 6**, blue and red data points, respectively). A non-linear response of activity (^{3}MLCT lifetime) with σ_p typically indicates a change in mechanism. Furthermore, the two different non-linear responses of τ_3 with σ_p observed here is in stark contrast with a recent study on Re(I)(terpyridine)$(CO)_3$ complexes whose ^{3}MLCT lifetime is linear with the σ_p of ligand substitution across a similar range.[48] However, for the Re(I) system, there is only one polypyridyl ligand where MLCT could localize, where for the **Cu-R** series there are two potential ligands for MLCT localization. Given the vast difference in excited-state decay mechanisms and kinetics of Cu(I)diimine complexes as a function of solvent,[7] we will discuss the trends in τ_3 with σ_p separately for CH_2Cl_2 and DMF.

In CH_2Cl_2, τ_3 is longest for **Cu-H** and decreases roughly linearly moving away from $\sigma_p = 0$. We interpret the sharp change in slope at $\sigma_p = 0$, resembling a volcano-plot type response, as confirmation of the change in directionality of MLCT as we go from R = H to either electron-donating or -withdrawing substituents. For all **Cu-R** the HOMO resides on the central copper atom, whereas the LUMO resides on the mesphen ligand for electron-donating phen substitution and on the 4,7-R-phen ligand for electron-withdrawing phen substitution (supported by DFT and CV in **Figures 2b**, **S28**, **S31**). For each set of **Cu-R** ($\sigma_p < 0$ or $\sigma_p > 0$), the roughly linear response of $\tau_3$with σ_p represents its own linear free energy relationship for MLCT to a specific coordinating ligand. We note that the lifetime for **Cu-CHO** is an outlier in this series, but as discussed above, the aldehyde groups introduce unusual reactivity in other solvents and there may be other electronic structure factors (specifically, as observed in the dramatic red-shift of the MLCT band) leading to the extremely fast decay of this ^{3}MLCT state. Nevertheless, the CH_2Cl_2 results demonstrate that we can use the ground state Hammett parameter to determine where the MLCT state is localized, and a simple linear relationship to predict the excited-state kinetics.

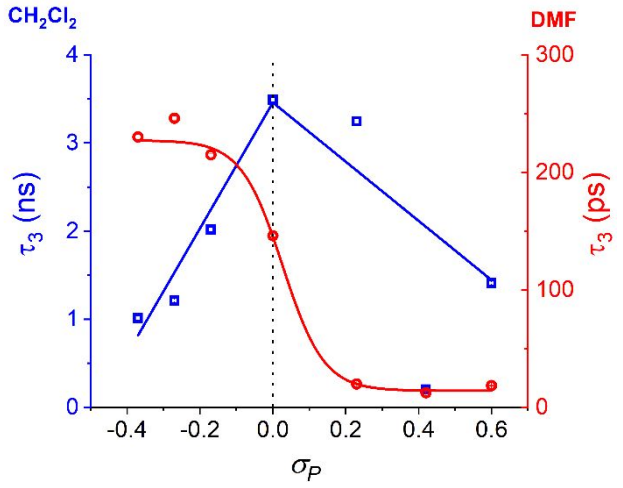

Figure 6. Plot of ^{3}MLCT lifetime for **Cu-R** as a function of σ_P in CH_2Cl_2 (left y-axis, blue squares) and DMF (right y-axis, red circles) and lines represent fits to data. Dashed line at $\sigma_p = 0$ to aid discussion; linear fits to CH_2Cl_2 data obtained by setting intercept to τ_3 value for **Cu-H**.

By contrast, in the strongly donating solvent DMF, τ_3 is longest and of similar magnitude for **Cu-R** with electron-donating substituents (210 – 250 ps), decreases sharply for **Cu-H**, and decreases even further with electron-withdrawing substituents, which are again of similar magnitude (10 – 20 ps). Given that the mesphen ligand is the constant for all of the **Cu-R**, and our experimental variable is the secondary phen ligand, this unusual response can be explained by the inductive effect of the R substituents that: 1) change the directionality of MLCT leading to localization of the LUMO and 2) stabilize (or de-stabilize) the formal Cu(II) center in the MLCT state. For **Cu-R** with electron-donating substitution, where $\sigma_p < 0$, CV and DFT calculations indicate that the LUMO is localized on the mesphen ligand. In the formal Cu(II) MLCT state we propose that the electron-donating substituents have a stabilizing inductive effect on the metal-centered HOMO by pushing electron density across the complex to localize on mesphen, creating an effective oxidation state that is between Cu(II) and Cu(I). This "less oxidized" HOMO then is stabilized in the typically strongly donating DMF by promoting weaker direct metal–solvent interactions by both a less dramatic flattening distortion or a less electrophilic Cu(I)-like center. Both steric and electronic factors would decrease the effect of the donor solvent and result in a more stabilized ^{3}MLCT state than for **Cu-H**, which we observe in the longer τ_3 values for **Cu-R** where $\sigma_p < 0$.

The inductive effect, in reverse, also explains the sharp decrease in τ_3 for **Cu-R** with $\sigma_p > 0$ where the LUMO is localized on the 4,7-R-phen ligand. We propose that the electron-withdrawing groups have a de-stabilizing effect on the metal-centered HOMO by pulling electron density away from the metal center and increasing the Cu(II) character. This highly electrophilic Cu(II) center then is susceptible to stronger interaction with DMF solvent molecules, leading to fast excited-state decay and the resulting short τ_3 values. A similar effect of electron-donating and –withdrawing substitution on the emission lifetime of functionalized Ru(II)bis(terpyridine) complexes was observed previously,[44] although in those complexes there is typically little to no direct interaction of the solvent with the excited state. With this **Cu-R** series, we uncovered the complex interplay of solvent interactions, excited-state structural reorganization, and ligand electronic structure to enable predictable excited-state activity using ground-state parameters.

Conclusions

In this work we used the HETPHEN approach to prepare seven heteroleptic Cu(I) photosensitizers and demonstrated the effect of the Hammett parameter of ligand substitution on their ground- and excited-state activity. The Cu(II/I) oxidation potential can be tuned over nearly 500 mV through the introduction of electron-donating or –withdrawing substituents, and the metal-centered couple follows a linear free energy relationship with σ_p of the ligand substituents. DFT and TD-DFT calculations were used to complement the experimental studies and illustrate that for complexes with electron-donating groups ($-0.37 < \sigma_p < 0$), the major contribution to the MLCT transition comes from charge transfer from the Cu(I) 3d orbital to the mesphen blocking ligand, while electron-withdrawing groups ($0 < \sigma_p < 0.6$) direct the MLCT transition to the secondary phenanthroline ligand. Analysis of the ultrafast transient absorption spectroscopy of this series reveals unexpected, non-linear trends in the ^{3}MLCT lifetime with σ_p which is different in coordinating and non-coordinating solvents. We interpret this activity as a direct outcome of the directionality of MLCT and localization of the charge separated state on just one of the ligands.

In the design of effective systems for harnessing and utilizing diffuse solar energy, it is imperative to understand where photoinduced charge-transfer states localize so that they can be extracted to provide electrons for productive redox chemistry. Recent elegant synthesis and spectroscopic studies have shown how to manipulate metal-to-ligand, ligand-to-metal, and ligand-centered charge-transfer states in coordination complexes based on first row transition metals to dramatically extend excited-state lifetimes.[49-55] The work presented here complements these studies by providing a foundational understanding of the directionality of MLCT states in earth-abundant molecular photosensitizers, potentially circumventing the need for extremely long-lived excited states because the photogenerated electrons are exactly where they need to be. Here we have shown that by adding common electron-donating or –withdrawing phenanthroline ligands we can predictively direct the MLCT state to one ligand or another. In this way, this work will contribute to the design of photocatalytic systems with high quantum efficiency where every photon absorbed produces a localized charge-transfer state of known thermodynamic properties and kinetic lifetimes that are predicted by the trends described here. Ongoing work in our group will utilize these design principles to integrate heteroleptic Cu(I)bis(phenanthroline) photosensitizers functionalized with substituents that promote localized MLCT states that

can be further carried on for use in multi-electron photoredox catalysis.

ASSOCIATED CONTENT

Supporting Information. General experimental methods and instrumentation; ligand and **Cu-R** synthesis and structural characterization; single crystal X-ray diffraction methods, additional figures and tabulated results; electrochemical methods and results; UV-Vis spectra; details of DFT and TD-DFT calculations and results; ultrafast transient absorption spectroscopy methods, detailed fitting information, and transient spectra and fitting details. This material is available free of charge via the Internet at http://pubs.acs.org.

AUTHOR INFORMATION

Corresponding Author

*mulfort@anl.gov

Author Contributions

The manuscript was written through contributions of all authors. All authors have given approval to the final version of the manuscript.

ACKNOWLEDGMENT

This work is supported by the Division of Chemical Sciences, Geosciences, and Biosciences, Office of Basic Energy Sciences of the U.S. Department of Energy through Contract No. DE-AC02-06CH11357. We gratefully acknowledge the computing resources provided on Bebop, a high-performance computing cluster operated by the Laboratory Computing Resource Center at Argonne National Laboratory.

REFERENCES

1. Ponseca, C. S.; Chábera, P.; Uhlig, J.; Persson, P.; Sundström, V., Ultrafast Electron Dynamics in Solar Energy Conversion. *Chemical Reviews* **2017,** *117* (16), 10940-11024.
2. Arias-Rotondo, D. M.; McCusker, J. K., The photophysics of photoredox catalysis: a roadmap for catalyst design. *Chem. Soc. Rev.* **2016**.
3. Hossain, A.; Bhattacharyya, A.; Reiser, O., Copper's rapid ascent in visible-light photoredox catalysis. *Science* **2019,** *364* (6439), eaav9713.
4. Concepcion, J. J.; House, R. L.; Papanikolas, J. M.; Meyer, T. J., Chemical approaches to artificial photosynthesis. *Proc. Natl. Acad. Sci. U. S. A.* **2012,** *109* (39), 15560-15564.
5. Zhang, B.; Sun, L., Artificial photosynthesis: opportunities and challenges of molecular catalysts. *Chem. Soc. Rev.* **2019,** *48* (7), 2216-2264.
6. Dalle, K. E.; Warnan, J.; Leung, J. J.; Reuillard, B.; Karmel, I. S.; Reisner, E., Electro- and Solar-Driven Fuel Synthesis with First Row Transition Metal Complexes. *Chemical Reviews* **2019,** *119* (4), 2752-2875.
7. Mara, M. W.; Fransted, K. A.; Chen, L. X., Interplays of excited state structures and dynamics in copper(I) diimine complexes: Implications and perspectives. *Coord. Chem. Rev.* **2015,** *282-283*, 2-18.
8. Kohler, L.; Hayes, D.; Hong, J.; Carter, T. J.; Shelby, M. L.; Fransted, K. A.; Chen, L. X.; Mulfort, K. L., Synthesis, structure, ultrafast kinetics, and light-induced dynamics of CuHETPHEN chromophores. *Dalton Trans.* **2016,** *45*, 9871-9883.
9. Kohler, L.; Hadt, R. G.; Hayes, D.; Chen, L. X.; Mulfort, K. L., Synthesis, structure, and excited state kinetics of heteroleptic Cu(i) complexes with a new sterically demanding phenanthroline ligand. *Dalton Trans.* **2017,** *46* (38), 13088-13100.
10. Lazorski, M. S.; Castellano, F. N., Advances in the light conversion properties of Cu(I)-based photosensitizers. *Polyhedron* **2014,** *82*, 57-70.
11. Sandroni, M.; Pellegrin, Y.; Odobel, F., Heteroleptic bis-diimine copper(I) complexes for applications in solar energy conversion. *Comptes Rendus Chimie* **2016,** *19* (1–2), 79-93.
12. Beaudelot, J.; Oger, S.; Peruško, S.; Phan, T.-A.; Teunens, T.; Moucheron, C.; Evano, G., Photoactive Copper Complexes: Properties and Applications. *Chemical Reviews* **2022,** *122* (22), 16365-16609.
13. Luo, S. P.; Mejía, E.; Friedrich, A.; Pazidis, A.; Junge, H.; Surkus, A. E.; Jackstell, R.; Denurra, S.; Gladiali, S.; Lochbrunner, S., Photocatalytic water reduction with copper-based photosensitizers: a noble-metal-free system. *Angew. Chem.* **2013,** *125* (1), 437-441.
14. Tschierlei, S.; Karnahl, M.; Rockstroh, N.; Junge, H.; Beller, M.; Lochbrunner, S., Substitution-Controlled Excited State Processes in Heteroleptic Copper (I) Photosensitizers Used in Hydrogen Evolving Systems. *ChemPhysChem* **2014,** *15* (17), 3709-3713.
15. Heberle, M.; Tschierlei, S.; Rockstroh, N.; Ringenberg, M.; Frey, W.; Junge, H.; Beller, M.; Lochbrunner, S.; Karnahl, M., Heteroleptic Copper Photosensitizers: Why an Extended π-System Does Not Automatically Lead to Enhanced Hydrogen Production. *Chemistry–A European Journal* **2017,** *23* (2), 312-319.
16. Giereth, R.; Frey, W.; Junge, H.; Tschierlei, S.; Karnahl, M., Copper photosensitizers containing P^ N ligands and their influence on photoactivity and stability. *Chemistry–A European Journal* **2017,** *23* (69), 17432-17437.
17. Liu, Y.; Yiu, S.-C.; Ho, C.-L.; Wong, W.-Y., Recent advances in copper complexes for electrical/light energy conversion. *Coord. Chem. Rev.* **2018,** *375*, 514-557.
18. Schmittel, M.; Ganz, A., Stable mixed phenanthroline copper(i) complexes. Key building blocks for supramolecular coordination chemistry. *Chemical Communications* **1997,** (11), 999-1000.
19. Schmittel, M.; Luning, U.; Meder, M.; Ganz, A.; Michel, C.; Herderich, M., Synthesis of sterically encumbered 2,9-diaryl substituted phenanthrolines. Key building blocks for the preparation of mixed (bis-heteroleptic) phenanthroline copper(I) complexes (I). *Heterocycl. Commun.* **1997,** *3* (6), 493-498.
20. De, S.; Mahata, K.; Schmittel, M., Metal-coordination-driven dynamic heteroleptic architectures. *Chem. Soc. Rev.* **2010,** *39* (5), 1555-1575.
21. Lazorski, M. S.; Gest, R. H.; Elliott, C. M., Photoinduced Multistep Charge Separation in a Heteroleptic Cu(I) Bis(phenanthroline)-Based Donor–Chromophore–Acceptor Triad. *Journal of the American Chemical Society* **2012,** *134* (42), 17466-17469.
22. Pellegrin, Y.; Sandroni, M.; Blart, E.; Planchat, A.; Evain, M.; Bera, N. C.; Kayanuma, M.; Sliwa, M.; Rebarz, M.; Poizat, O.; Daniel, C.; Odobel, F., New Heteroleptic Bis-Phenanthroline Copper(I) Complexes with Dipyridophenazine or Imidazole Fused Phenanthroline Ligands: Spectral, Electrochemical, and Quantum Chemical Studies. *Inorg. Chem.* **2011,** *50* (22), 11309-11322.
23. Sandroni, M.; Favereau, L.; Planchat, A.; Akdas-Kilig, H.; Szuwarski, N.; Pellegrin, Y.; Blart, E.; Le Bozec, H.; Boujtita, M.; Odobel, F., Heteroleptic copper(I)-polypyridine complexes as efficient sensitizers for dye sensitized solar cells. *J. Mater. Chem. A* **2014,** *2* (26), 9944-9947.
24. Hayes, D.; Kohler, L.; Chen, L. X.; Mulfort, K. L., Ligand Mediation of Vectorial Charge Transfer in Cu(I)diimine Chromophore–Acceptor Dyads. *J. Phys. Chem. Lett.* **2018,** *9* (8), 2070-2076.
25. Hayes, D.; Kohler, L.; Hadt, R. G.; Zhang, X.; Liu, C.; Mulfort, K. L.; Chen, L. X., Excited state electron and energy relays in supramolecular dinuclear complexes revealed by ultrafast optical and X-ray transient absorption spectroscopy. *Chemical science* **2018,** *9* (4), 860-875.

26. Mara, M. W.; Phelan, B. T.; Xie, Z.-L.; Kim, T. W.; Hsu, D. J.; Liu, X.; Valentine, A. J. S.; Kim, P.; Li, X.; Adachi, S.-i.; Katayama, T.; Mulfort, K. L.; Chen, L. X., Unveiling ultrafast dynamics in bridged bimetallic complexes using optical and X-ray transient absorption spectroscopies. *Chemical Science* **2022,** *13* (6), 1715-1724.

27. Sandroni, M.; Kayanuma, M.; Planchat, A.; Szuwarski, N.; Blart, E.; Pellegrin, Y.; Daniel, C.; Boujtita, M.; Odobel, F., First application of the HETPHEN concept to new heteroleptic bis(diimine) copper(i) complexes as sensitizers in dye sensitized solar cells. *Dalton Trans.* **2013,** *42* (30), 10818-10827.

28. Eberhart, M. S.; Phelan, B. T.; Niklas, J.; Sprague-Klein, E. A.; Kaphan, D. M.; Gosztola, D. J.; Chen, L. X.; Tiede, D. M.; Poluektov, O. G.; Mulfort, K. L., Surface immobilized copper(i) diimine photosensitizers as molecular probes for elucidating the effects of confinement at interfaces for solar energy conversion. *Chemical Communications* **2020,** *56* (81), 12130-12133.

29. Chen, L. X.; Jager, W. J. H.; Jennings, G.; Gosztola, D. J.; Munkholm, A.; Hessler, J. P., Capturing a Photoexcited Molecular Structure Through Time-Domain X-ray Absorption Fine Structure. *Science* **2001,** *292* (5515), 262-264.

30. Iwamura, M.; Takeuchi, S.; Tahara, T., Real-Time Observation of the Photoinduced Structural Change of Bis(2,9-dimethyl-1,10-phenanthroline)copper(I) by Femtosecond Fluorescence Spectroscopy: A Realistic Potential Curve of the Jahn–Teller Distortion. *Journal of the American Chemical Society* **2007,** *129* (16), 5248-5256.

31. Scaltrito, D. V.; Thompson, D. W.; O'Callaghan, J. A.; Meyer, G. J., MLCT excited states of cuprous bis-phenanthroline coordination compounds. *Coord. Chem. Rev.* **2000,** *208* (1), 243-266.

32. Dietrich-Buchecker, C. O. M., P. A.; Sauvage, J.-P.; Kirchhoff, J. R.; McMillin, D. R., Bis(2,9-diphenyl-1,10-phenanthroline)copper(I): a Copper Complex with a Long-lived Charge-transfer Excited State. *J. Chem. Soc. Chem. Commun.* **1983**, 513-515.

33. Eggleston, M. K.; McMillin, D. R.; Koenig, K. S.; Pallenberg, A. J., Steric Effects in the Ground and Excited States of Cu(NN)2+ Systems. *Inorg. Chem.* **1997,** *36* (2), 172-176.

34. Cuttell, D. G.; Kuang, S.-M.; Fanwick, P. E.; McMillin, D. R.; Walton, R. A., Simple Cu (I) complexes with unprecedented excited-state lifetimes. *Journal of the American Chemical Society* **2002,** *124* (1), 6-7.

35. Phifer, C. C.; McMillin, D. R., The basis of aryl substituent effects on charge-transfer absorption intensities. *Inorg. Chem.* **1986,** *25* (9), 1329-1333.

36. Green, O.; Gandhi, B. A.; Burstyn, J. N., Photophysical Characteristics and Reactivity of Bis(2,9-di-tert-butyl-1,10-phenanthroline)copper(I). *Inorg. Chem.* **2009,** *48* (13), 5704-5714.

37. Schmittel, M.; Ganz, A.; Fenske, D.; Herderich, M., Heteroleptic silver (I) and zinc (II) bis (phenanthroline) complexes. *Journal of the Chemical Society, Dalton Transactions* **2000,** (3), 353-359.

38. Fraser, M. G.; van der Salm, H.; Cameron, S. A.; Blackman, A. G.; Gordon, K. C., Heteroleptic Cu(I) Bis-diimine Complexes of 6,6 '-Dimesityl-2,2 '-bipyridine: A Structural, Theoretical and Spectroscopic Study. *Inorg. Chem.* **2013,** *52* (6), 2980-2992.

39. Yang, L.; Powell, D. R.; Houser, R. P., Structural variation in copper (I) complexes with pyridylmethylamide ligands: structural analysis with a new four-coordinate geometry index, τ 4. *Dalton Trans.* **2007,** (9), 955-964.

40. Dickenson, J. C.; Haley, M. E.; Hyde, J. T.; Reid, Z. M.; Tarring, T. J.; Iovan, D. A.; Harrison, D. P., Fine-Tuning Metal and Ligand-Centered Redox Potentials of Homoleptic Bis-Terpyridine Complexes with 4′-Aryl Substituents. *Inorg. Chem.* **2021,** *60* (13), 9956-9969.

41. Lanznaster, M.; Neves, A.; Bortoluzzi, A. J.; Assumpção, A. M. C.; Vencato, I.; Machado, S. P.; Drechsel, S. M., Electronic Effects of Electron-Donating and -Withdrawing Groups in Model Complexes for Iron-Tyrosine-Containing Metalloenzymes. *Inorg. Chem.* **2006,** *45* (3), 1005-1011.

42. Masui, H.; Lever, A. B. P., Correlations between the ligand electrochemical parameter, EL(L), and the Hammett substituent parameter, .sigma. *Inorg. Chem.* **1993,** *32* (10), 2199-2201.

43. Simón-Manso, Y., Linear Free-Energy Relationships and the Density Functional Theory: An Analog of the Hammett Equation. *J. Phys. Chem. A* **2005,** *109* (9), 2006-2011.

44. Maestri, M.; Armaroli, N.; Balzani, V.; Constable, E. C.; Thompson, A. M. W. C., Complexes of the Ruthenium(II)-2,2':6',2''-terpyridine Family. Effect of Electron-Accepting and -Donating Substituents on the Photophysical and Electrochemical Properties. *Inorg. Chem.* **1995,** *34* (10), 2759-2767.

45. Martin, R. L., Natural transition orbitals. *The Journal of chemical physics* **2003,** *118* (11), 4775-4777.

46. Yu, H. S.; Li, S. L.; Truhlar, D. G., Perspective: Kohn-Sham density functional theory descending a staircase. *The Journal of chemical physics* **2016,** *145* (13), 130901.

47. Iwamura, M.; Takeuchi, S.; Tahara, T., Ultrafast Excited-State Dynamics of Copper(I) Complexes. *Acc. Chem. Res.* **2015,** *48* (3), 782-791.

48. Fernández-Terán, R.; Sévery, L., Living Long and Prosperous: Productive Intraligand Charge-Transfer States from a Rhenium(I) Terpyridine Photosensitizer with Enhanced Light Absorption. *Inorg. Chem.* **2021,** *60* (3), 1334-1343.

49. Liu, Y.; Harlang, T.; Canton, S. E.; Chábera, P.; Suárez-Alcántara, K.; Fleckhaus, A.; Vithanage, D. A.; Göransson, E.; Corani, A.; Lomoth, R.; Sundström, V.; Wärnmark, K., Towards longer-lived metal-to-ligand charge transfer states of iron(ii) complexes: an N-heterocyclic carbene approach. *Chemical Communications* **2013,** *49* (57), 6412-6414.

50. Liu, L.; Duchanois, T.; Etienne, T.; Monari, A.; Beley, M.; Assfeld, X.; Haacke, S.; Gros, P. C., A new record excited state 3MLCT lifetime for metalorganic iron(ii) complexes. *Physical Chemistry Chemical Physics* **2016,** *18* (18), 12550-12556.

51. Wenger, O. S., Photoactive Complexes with Earth-Abundant Metals. *Journal of the American Chemical Society* **2018,** *140* (42), 13522-13533.

52. Yarranton, J. T.; McCusker, J. K., Ligand-Field Spectroscopy of Co(III) Complexes and the Development of a Spectrochemical Series for Low-Spin d6 Charge-Transfer Chromophores. *Journal of the American Chemical Society* **2022,** *144* (27), 12488-12500.

53. Ogawa, T.; Sinha, N.; Pfund, B.; Prescimone, A.; Wenger, O. S., Molecular Design Principles to Elongate the Metal-to-Ligand Charge Transfer Excited-State Lifetimes of Square-Planar Nickel(II) Complexes. *Journal of the American Chemical Society* **2022,** *144* (48), 21948-21960.

54. Leary, D. C.; Martinez, J. C.; Akhmedov, N. G.; Petersen, J. L.; Milsmann, C., Long-lived photoluminescence from an eight-coordinate zirconium(iv) complex with four 2-(2′-pyridyl)pyrrolide ligands. *Chemical Communications* **2022,** *58* (85), 11917-11920.

55. Rosko, M. C.; Espinoza, E. M.; Arteta, S.; Kromer, S.; Wheeler, J. P.; Castellano, F. N., Employing Long-Range Inductive Effects to Modulate Metal-to-Ligand Charge Transfer Photoluminescence in Homoleptic Cu(I) Complexes. *Inorg. Chem.* **2023,** *62* (7), 3248-3259.

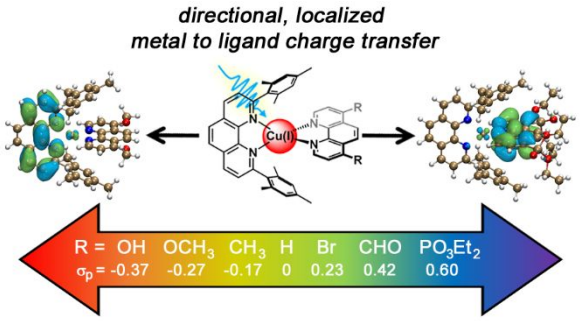

Synopsis: A Hammett series of heteroleptic Cu(I)bis(phenanthroline) complexes was investigated to determine the directionality and kinetics of metal-to-ligand charge transfer in response to ligand electronics and solvent environment. Experimental and computational analyses confirm that MLCT is localized on only one ligand, which is dictated by the electron-donating or –withdrawing character of the substituents. The inductive effect of the phenanthroline substituents influences solvent interactions in the MLCT state with dramatic implications for the excited state lifetime.